IOPscience iopscience.iop.org

Home Search Collections Journals About Contact us My IOPscience

Structure and properties of amorphous silicon-metal alloys: I. The $Si_{1-x}Ni_x$ system

This article has been downloaded from IOPscience. Please scroll down to see the full text article.

2000 J. Phys.: Condens. Matter 12 5971

(http://iopscience.iop.org/0953-8984/12/27/315)

View the table of contents for this issue, or go to the journal homepage for more

Download details:
IP Address: 171.66.16.221
The article was downloaded on 16/05/2010 at 05:19

Please note that terms and conditions apply.

J. Phys.: Condens. Matter **12** (2000) 5971–5980. Printed in the UK PII: S0953-8984(00)12205-2

Structure and properties of amorphous silicon–metal alloys: I. The $Si_{1-x}Ni_x$ system

B T Williams, S J Gurman, S H Baker and E A Davis
Department of Physics and Astronomy, University of Leicester, Leicester LE1 7RH, UK

Received 1 March 2000

Abstract. Structural and optical measurements have been made on a series of amorphous thin films of $Si_{1-x}Ni_x$ with $0 < x < 0.75$, prepared by RF sputtering. We present the results of structural studies using extended x-ray absorption fine structure (EXAFS) and small angle x-ray scattering (SAXS) together with optical measurements of the band gap.

The EXAFS analysis gave interatomic distances, partial coordination numbers and Debye–Waller factors for the nearest neighbours of the two atom types. The Ni environment was found to be independent of composition for $x < 0.5$. A small variation in the mean Si–Si distance was also found in this composition range. The SAXS results show phase segregation, on the 30 Å scale, for this composition range. We interpret the structural data in terms of a two-phase model, amorphous Si plus amorphous NiSi, for $x < 0.5$ and a single-phase model for $x > 0.5$.

The optical data show that a metal–insulator transition occurs at about 10–15% Ni content. We suggest that this transition should be interpreted in terms of a percolation theory involving regions of conducting amorphous NiSi in an amorphous Si matrix.

1. Introduction

Transition metal silicides have been studied in depth to enhance the understanding of the metal to insulator transition (MIT) and because of their potential device application. Amorphous samples are particularly convenient for MIT studies since their composition can be varied smoothly over a wide composition range. As device dimensions decreased, it became clear that the resistance of conductors fabricated from polycrystalline silicon would become too high. The resistivity of pure silicon can be varied across a large range, however, by progressively adding metal and hence the tailoring of its conductive properties becomes possible.

The electronic behaviour of the a-Si:metal system has been studied in depth [1], although ideas about the mechanism of the MIT are changing and the value of critical metal content, N_c, at which the MIT occurs is often not well characterized. Under the condition that metal atoms substitute randomly into the tetrahedral random network (TRN) of amorphous silicon, the MIT can be thought of in terms of the extension of localized states [2]. It was originally assumed that these amorphous materials were structurally homogeneous but recent investigations have shown that inhomogeneities exist, upsetting the idea of a random distribution, and hence a percolation theory may be more appropriate to model the MIT [3].

Studies performed on a-$Si_{1-x}Ni_x$ generally agree that the MIT occurs at between 10 and 20 at.% nickel [4, 5] although Rogachev *et al* [6] have noted a dramatic decrease in the width of the optical band gap after addition of only 5 at.% nickel.

Investigations into the atomic structure of *hydrogenated* samples have been carried out by two groups [7, 8], both of whom find that the inclusion of Ni in a-Si leads to local re-ordering

0953-8984/00/275971+10$30.00 © 2000 IOP Publishing Ltd

of the TRN and suggest clusters of a separate Ni:Si phase form within a-SiNi:H, implying that a percolation model would indeed be an appropriate description of the transport behaviour. This conclusion has been reinforced with SAXS experiments performed on the same system [9]. The identity of the Ni:Si phase was not identified in any of this work, which was mainly limited to low ($x < 0.3$) nickel content materials [7, 9].

Originally, a detailed understanding of the local atomic structure of a material was thought necessary to fathom the MIT. It now looks as though an understanding of the mid-range structure is equally important. It is with this in mind that we present here the combined results from EXAFS and SAXS experiments performed on a series of a-$Si_{1-x}Ni_x$ samples, where $0.00 \leqslant x \leqslant 0.74$.

2. Sample preparation

Thin films of amorphous $Si_{1-x}Ni_x$, approximately 1 μm thick, were prepared by RF sputtering using a Nordiko NM-2000-T8-SE1 system. The pressure during sputtering was about 5 mTorr and the power applied to the target 200 W at a frequency of 13.56 MHz. The target consisted of a 10 cm disc of silicon with a number of squares of nickel foil placed on it. The number of these pieces was varied in order to vary the composition of the sputtered alloy. A variety of substrates was included in each deposition run: Mylar and copper foil for the EXAFS samples, aluminium foil for the SAXS samples and Corning 7059 glass for the optical samples.

The sample composition was determined using energy-dispersive x-ray analysis in a DS 130 scanning electron microscope. This method determines x to about ± 0.02, judging by the scatter of values obtained from different parts of the sample. All samples were found to contain about 2% argon, from the sputtering gas. The amorphicity of the samples was checked by transmission electron microscopy using a JEOL 100 CX instrument.

3. Experimental details and data analysis

EXAFS and SAXS measurements on the samples were performed on the synchrotron radiation source at the CLRC Daresbury Laboratory. The synchrotron was running at an electron energy of 2 GeV and beam currents of 150–250 mA during all experiments.

3.1. EXAFS measurements

The Si K edge was measured on station 3.4. This station has a chromium plated pre-mirror which provides a high energy x-ray cut-off at about 4 keV to minimize harmonic contamination. The energy of the x-ray beam was defined using an InSb(111) double-crystal monochromator. Absorption at the sample was measured by the electron drain current method: for this technique to be used the samples must be deposited on a conducting (here copper) substrate. The Ni K-edge data were taken on station 7.1 using the standard transmission geometry. This station has a silicon(111) double-crystal monochromator. Harmonic rejection was achieved by a 50% detuning off the Bragg peak. Sample absorption was measured using two ion chambers filled with an Ar/He gas mixture, the compositions being set to give 20% absorption for the I_0 monitor and 80% absorption for the I_t monitor. The absorption step at the Ni K edge was set close to unity by folding the samples to give the appropriate amount of nickel in the beam. For this reason these samples were deposited on thin Mylar substrates.

3.2. SAXS measurements

SAXS measurements were made on station 8.2. This provides a highly collimated x-ray beam of wavelength 1.5 Å from a Ge(111) monochromator. The detector was a 512-wire proportional counter, the quadrant detector, with a maximum count rate of 10^5 photons s^{-1}. A camera length of 1.5 m was used so that the maximum scattering vector measured was 0.5 $Å^{-1}$. The first 0.02 $Å^{-1}$ of this range is obscured by a beam stop, to prevent the direct beam from overloading the detector. The scattering vector was calibrated using a standard collagen sample. Each SAXS spectrum results from a 2 min collecting time. Aluminium substrates were used for the SAXS samples, since these give a smooth background in the SAXS region.

3.3. Optical measurements

Optical measurements at visible and near infra-red photon energies were made using a double-beam Perkin–Elmer 330 instrument. The absorption coefficient α and refractive index $n(E)$ were determined by standard transmission and reflection methods.

3.4. Data analysis

The EXAFS data were calibrated, background subtracted and analysed using standard Daresbury packages, EXCALIB, EXBACK and EXCURV92 respectively. EXCALIB converts monochromator positions to x-ray energy and the detector signals to an absorption coefficient. EXBACK fits the pre- and post-edge regions by low-order polynomials in the standard manner to extract the oscillatory EXAFS function.

The package EXCURV92 uses a least-squares curve-fitting procedure to compare theoretical and experimental spectra, with the structural parameters (distance, co-ordination number, Debye–Waller factor and atom type) of the near neighbours as fitting parameters. The theoretical spectra were calculated using fast curved wave theory [10], including single scattering only. The Hedin–Lundqvist exchange potential and von Barth ground state potential were used to calculate the scattering phase-shifts for both edges. A standard Ni foil was used to determine the amplitude reduction factor (AFAC) to be used during analysis of Ni K-edge data: this was found to be 0.9. AFAC for the Si K edge was found to be 0.95 using the a-Si sample, where a coordination of four is expected, as a standard. The Hedin–Lundqvist potential is known to give a good description of inelastic processes in the EXAFS energy range, so AFAC should be very close to unity. The program also determines the uncertainties in the fitted parameters and also determines whether a shell of atoms *significantly* improves the fit, using the Joyner method [11]. The uncertainties quoted here are always $\pm 2\sigma$ (95% confidence). All shells described improved the fit index significantly.

SAXS data reduction used the Daresbury XOTOKO package, which normalizes, calibrates and background subtracts the data. Most of the background comes from the substrate with some contribution from windows and air scatter: background subtraction used data from a blank aluminium substrate to deal with all of these. The data were analysed in terms of Guinier theory for the low-q structure (due to isolated structures) and a simple correlation length method for the high-q structure, which we believe to be due to phase segregation.

The optical analysis was based entirely on the measured absorption coefficient α. Two methods were used to determine the band gap: choice of a standard absorption and a Tauc analysis. The standard absorption used to define the band gap was $\alpha = 10^4$ cm^{-1}. The Tauc analysis assumes parabolic forms for the band edges and so derives the expression

$$E\alpha(E) = C(E - E_T)^2$$

for the energy variation of the absorption coefficient close to the absorption edge. The Tauc energy E_T, obtained from a plot of $(E\alpha)^{1/2}$ against E is then a measure of the band gap. The two analyses give very similar results for the optical band gap.

4. EXAFS, SAXS and optical results

4.1. EXAFS results

The results of the EXAFS analysis are shown in table 1, which gives the fitted values of the bond lengths R_{ij}, the partial coordination numbers N_{ij} and the mean square variations in distance (the EXAFS Debye–Waller factor) σ_{ij}^2. The structural parameters for the Ni–Si coordination obtained from analysis of the Ni and Si edge data are always consistent ($R_{NiSi} = R_{SiNi}$, $\sigma_{NiSi}^2 = \sigma_{SiNi}^2$ and $xN_{NiSi} = (1-x)N_{SiNi}$) within their uncertainties. These results are also consistent with those previously reported [7, 8] for low-nickel samples.

Table 1. EXAFS results for amorphous $Si_{1-x}Ni_x$ thin films. The uncertainties quoted are 2σ (95% confidence).

x	R (Å) (SiSi)	R (Å) (SiNi)	R (Å) (NiSi)	R (Å) (NiNi)	N (SiSi)	N (SiNi)	N (NiSi)	N (NiNi)	σ^2 (Å^2) (SiSi)	σ^2 (Å^2) (SiNi)	σ^2 (Å^2) (NiSi)	σ^2 (Å^2) (NiNi)
0.00	2.34	—	—	—	4.0	—	—	—	60	—	—	—
0.12	2.32	2.35	2.33	2.53	2.5	0.9	6.5	1.8	60	110	120	150
0.22	2.39	2.30	2.34	2.53	2.3	1.9	6.7	2.4	120	110	120	160
0.28	2.43	2.32	2.34	2.55	1.4	2.0	6.3	2.2	140	200	140	150
0.42	2.41	2.32	2.34	2.52	3.4	6.1	6.8	1.8	40	100	80	200
0.43	2.44	2.34	2.34	2.49	3.6	8.6	6.6	1.3	40	120	60	130
0.48	2.43	2.33	2.34	2.47	2.6	4.2	6.9	1.4	50	100	60	140
0.56	2.44	2.33	2.33	2.49	2.9	9.8	6.5	1.9	40	140	80	160
0.61	2.44	2.33	2.35	2.55	1.2	7.3	5.9	2.7	60	160	100	130
0.74	2.44	2.35	2.37	2.56	0.3	5.5	4.8	6.2	50	140	100	180
									$\times 10^{-4}$	$\times 10^{-4}$	$\times 10^{-4}$	$\times 10^{-4}$
	±0.02	±0.02	±0.02	±0.02	±0.5	±1.0	±0.5	±0.5	±30	±30	±30	±30

We note that the nickel environment is invariant, in R, N and σ, for all samples with $x < 0.5$. This is apparent in the EXAFS on the nickel K edge, shown as figure 1, which is very similar for all these samples. At higher nickel contents, the partial Ni coordinations vary, although the distances and mean square variations are still largely invariant, showing a fall-off in Ni–Si coordination as is to be expected as the silicon content of the samples falls to zero. The Si–Si distance rises from 2.34 to 2.44 Å in the composition range $x < 0.5$, staying constant thereafter. This is a significant variation since bond lengths in amorphous solids are generally found to vary very little with composition, particularly for covalent bonds. The mean square variation in distance shows a distinct peak at about 25% nickel content. The Si–Ni coordination number rises with increasing nickel content, in order to maintain consistency with the constant Ni–Si values for $x < 0.5$, but the mean square variation is probably invariant.

4.2. SAXS results

Figure 2(a) shows the background subtracted, normalized SAXS profile from seven of the samples studied, all of which display a large peak at $k = 0.030$ Å^{-1}, truncated at low k by the beam stop.

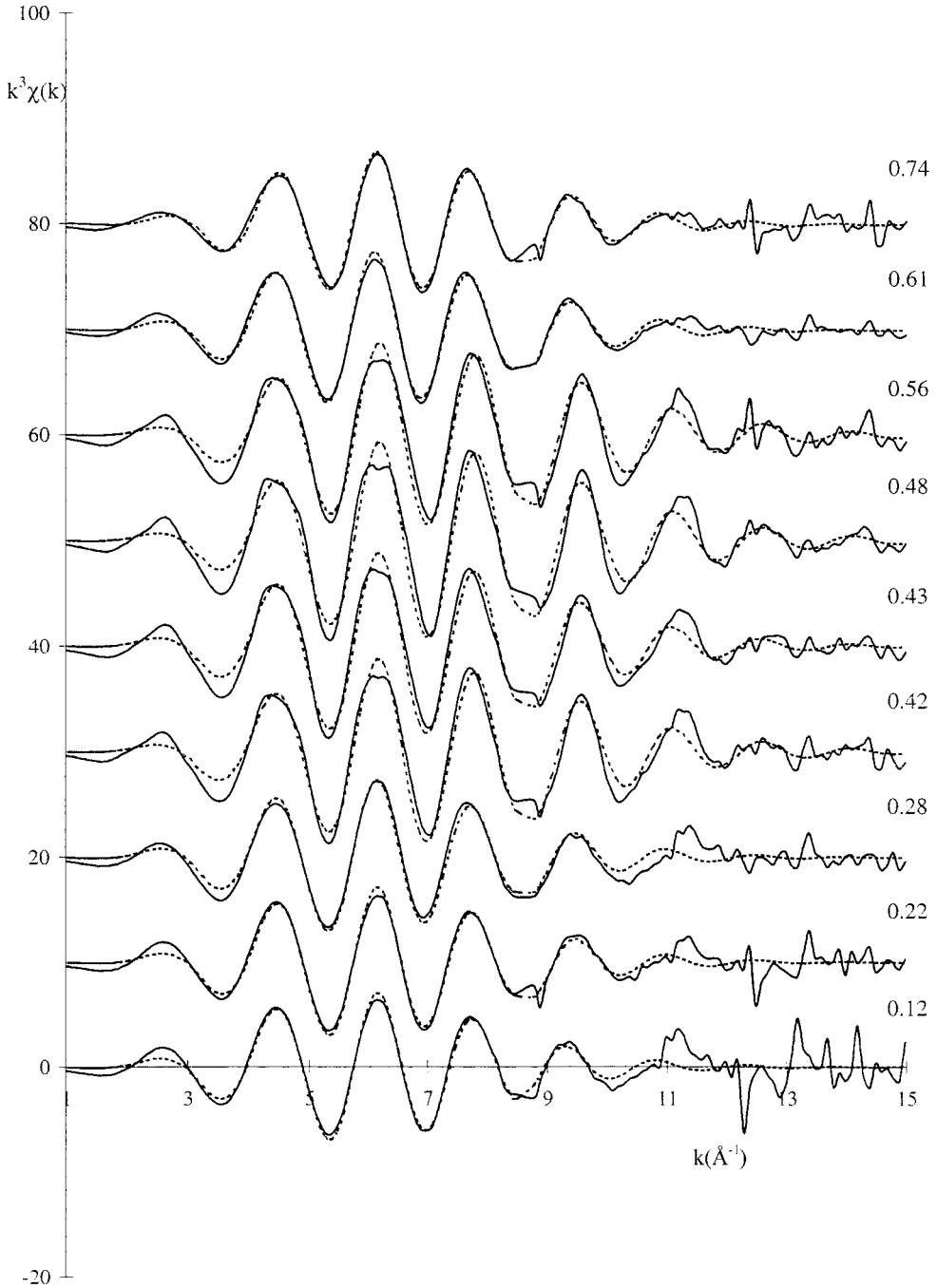

Figure 1. EXAFS spectra on the nickel K edge from amorphous $Si_{1-x}Ni_x$. Note the strong similarity between these spectra, especially for $x < 0.5$. Solid lines: experimental data, dashed lines: theoretical fits.

The relative amplitude of this Guinier peak gives an idea as to the relative number of scattering bodies incorporated in each sample. This is largely independent of composition

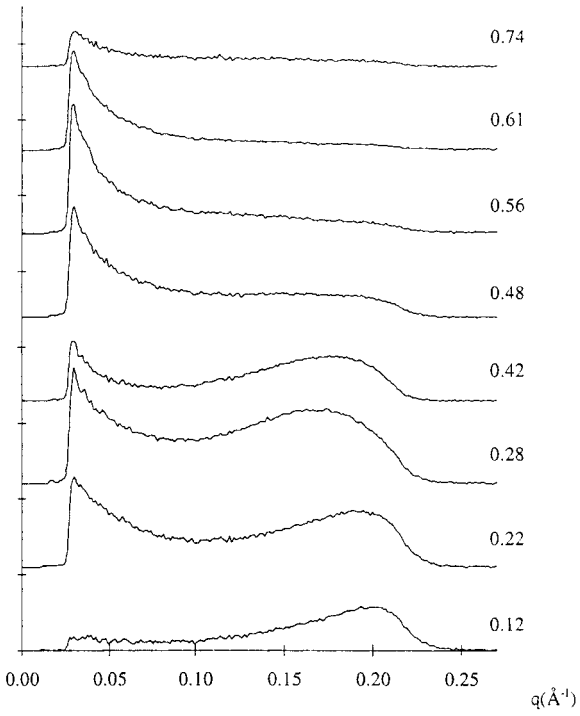

(a)

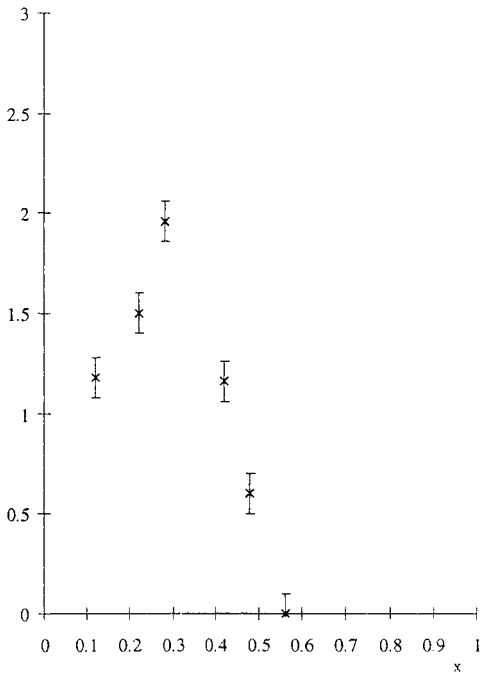

(b)

Figure 2. (a) Normalized and background-subtracted SAXS data for all samples except $x = 0.0$ and $x = 0.43$, labelled by x, the composition variable. (b) Amplitude of the SAXS peak at about $k = 0.18$ Å^{-1} as a function of nickel content.

suggesting that it is due to the presence of voids introduced during fabrication, as void characteristics are a function of deposition conditions rather than chemical composition. Guinier analysis [12] shows these inhomogeneities to have a radius of 45 ± 5 Å, for all compositions. We therefore identify this contribution as due to argon gas bubbles (all samples contain about 2% Ar) introduced during the sputtering process.

Samples in the range $0.12 \leqslant x \leqslant 0.48$ also show a second peak at higher k. This is caused by interference of x-rays scattered from non-disperse regions of contrasting electron density, e.g. between void and matrix or between regions of different phase. The relative amplitude of the observed second peak is composition dependent, suggesting that separation of the sample into distinct phases is taking place. The chemical composition of each phase can be inferred from an end-point analysis, shown in figure 2(b). The peak at 20–30 at.% Ni indicates the presence of two phases in similar quantities, while the disappearance of the peak at ∼50 at.% Ni points towards a single phase of a-NiSi. These results suggest the co-existence of a-NiSi and a-Si in the composition range $0.12 \leqslant x \leqslant 0.48$.

The angular position of the second peak, k_p, is related to the correlation length, L_c, of the scattering bodies by $L_c = 2\pi/k_p$. This distance lies between 0.19 and 0.16 Å^{-1}, corresponding to a correlation length of 33–40 Å, with a tendency to fall with increasing nickel content.

4.3. Optical results

We have measured the optical absorption spectrum of all samples with the aim of identifying the concentration at which a-$Si_{1-x}Ni_x$ ceases to be semiconducting and becomes metallic, recognised as the point at which the optical band gap closes. By measuring the absorption at optical wavelengths, the size of the band gap can be characterized; an absorption edge indicates the presence of a gap whereas constant absorption in this range implies a continuum and hence metallic behaviour. Two samples were found to display absorption edges, a-Si and the sample containing 12 at.% Ni, while flat, featureless curves were observed for all samples where $x \geqslant 0.22$. This implies that samples at and above 22 at.% Ni are metallic. The position of the MIT can be found by quantifying the gap in one of two ways:

(i) The energy when $\alpha(E)$ falls to a value of 10^4 cm^{-1} is taken, denoted by E_{04}. This method gave values of 1.4 ± 0.2 eV and 0.1 ± 0.2 eV for the band gaps of a-Si and a-$Si_{0.88}Ni_{0.12}$ respectively. The gap in crystalline Si is usually quoted as 1.2 eV [16], in agreement with that found for a-Si, although a slightly smaller band gap is expected in amorphous solids in relation to their crystalline counterparts because of disorder induced tailing of states into the gap.

(ii) Tauc analysis can be applied, where $\{\omega\alpha(E)\}^{1/2}$ against E is plotted, so that the intercept on the x-axis gives a value, E_{Tauc}, for the gap. Using Tauc analysis the band gap was found to be 1.3 ± 0.2 eV and 0.2 ± 0.2 eV for a-Si and a-$Si_{0.88}Ni_{0.12}$ respectively. The theory behind the Tauc gap assumes parabolic band edges, which may not be the case, especially when the band gap is very narrow so that band tails may overlap. Clearly, the MIT occurs at a composition just above $x = 0.12$. We have too few samples in the critical composition range to clearly define the position of the MIT. Our results are consistent with earlier studies [4, 5], in particular with our conductivity study [5] of samples prepared in exactly the same way as those used here. This earlier work used many more samples and gave a MIT close to 18% nickel content.

5. Discussion

Ni K-edge data show that, for $x < 0.5$, Ni atoms are surrounded by 6.5 ± 0.5 Si atoms at 2.34 ± 0.01 Å and 2.0 ± 0.5 Ni atoms at 2.50 ± 0.05 Å. These high coordination numbers imply that Ni does not substitute into the tetrahedral random network of a-Si as previously thought but exists only within the fairly close-packed structure of an amorphous Ni:Si alloy. However, Si K-edge data show Si as being fourfold coordinated at low metal content, consistent with the idea of a tetrahedral random network. These observations can be reconciled by invoking the idea of a two-phase system, with an a-Si:Ni alloy growing within an a-Si matrix. This idea is supported by results from the SAXS study which clearly show the presence of two non-disperse scattering media, of which one steadily increases in abundance until it dominates the sample at $x \sim 0.50$. This behaviour would be exhibited by samples containing regions of the phase NiSi within an a-Si network. Crystalline NiSi alloys have been observed to form from the melt [13]. We found no evidence of crystallization (i.e. no second peaks in the Fourier transform of the EXAFS spectra) at any composition, confirming that all phases present are amorphous.

Another group [7] working with the a-$Si_{1-x}Ni_x$:H system with $x < 0.3$ have observed the clustering of Ni atoms in the form of an amorphous Ni:Si alloy and have suggested that this alloy is a-$NiSi_2$. We report similarities in bond length and coordination number with those reported by Edwards *et al* [7]. However, our SAXS data strongly suggest that the Ni:Si inclusion has the composition NiSi, the phase segregation occurring on the 30–40 Å scale.

We can understand all of the structural data for $x < 0.5$ using a two-phase model. The nickel environment for $x < 0.5$ is that of the NiSi phase, so that the nearest neighbour parameters are independent of composition. The silicon environment is a mixture of amorphous Si ($R = 2.34$ Å, $N = 4$, $\sigma^2 = 60 \times 10^{-4}$ Å^2) and the amorphous NiSi phase. If we take this to have the nearest neighbour parameters $R_{SiSi} = 2.44$ Å, $N_{SiSi} = 2$, $R_{SiNi} = 2.32$ Å, $N_{SiNi} = 7$ (and $R_{NiNi} = 2.53$ Å and $N_{NiNi} = 2$) then we obtain a good fit to the data, as shown in figure 3. In particular, the varying Si–Si distance comes out of this model in a natural way. The distances and coordinations chosen are very similar to those found in crystalline NiSi [14]. This two-phase model, with two different Si–Si distances, will also lead to a roughly parabolic variation of the mean square variation of the Si–Si distance (but no other) as is actually observed, although the model will only give a maximum variation in σ^2_{SiSi} of about 40×10^{-4} Å^2, rather less than that observed.

For $x > 0.5$, R_{ij} and σ^2_{ij} are essentially constant for all bonds. Both Ni and Si are reasonably close packed and the coordination numbers suggest that chemical order is almost complete. The interatomic distances are similar to those seen in crystalline nickel silicides. We suggest that our samples are behaving as typical (metallic) amorphous metal–metalloid alloys in this composition range.

The measured Debye–Waller factors arise from a combination of thermal and static disorder. The room-temperature thermal contribution to the Si–Si Debye–Waller factor is about 40×10^{-4} Å^2 [15]. Our results suggest a small contribution from static disorder of about $(20–40) \times 10^{-4}$ Å^2 plus the contribution from the two Si–Si mean distances noted above. The Si–Ni Debye–Waller factor is found to be independent of composition at about $(100–150) \times 10^{-4}$ Å^2. The room-temperature thermal contribution, calculated using a method proposed by Cyrin [16] with a stretch frequency of 680 cm^{-1} [8], is only 30×10^{-4} Å^2 so this bond shows a considerable degree of static disorder. Using the Debye theory [17] to calculate the room-temperature thermal contribution to the Debye–Waller factor of the Ni–Ni bond gives a value of 40×10^{-4} Å^2 if the Debye temperature is taken to be 450 K [18]. Again our results indicate a large degree of static disorder, of the order of 0.1 Å RMS, in this interatomic distance.

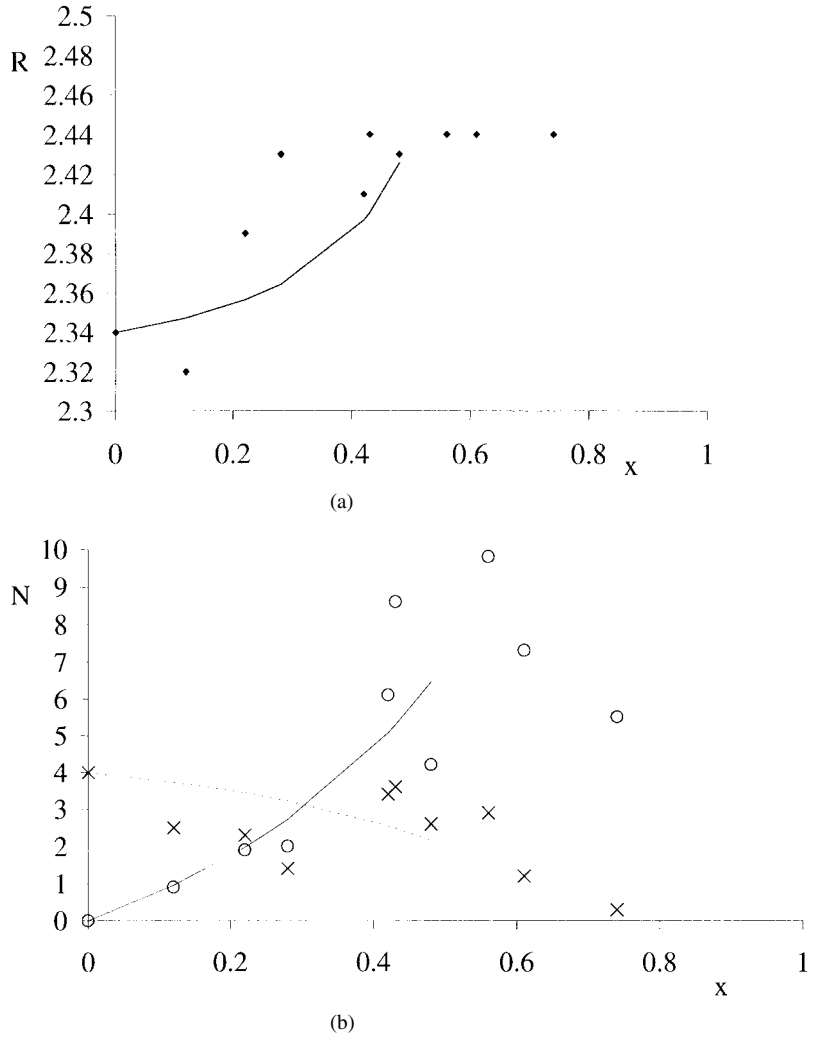

Figure 3. (a) Measured Si–Si distances (♦) and model predictions (line). See the text for a description of the model. (b) Measured Si–Si (×) and Si–Ni (○) partial coordination numbers and model predictions (dashed line Si–Si, solid line Si–Ni).

The presence of phase separation will clearly affect the MIT. We observe this event at about 10–15 at.% Ni, in fair agreement with the work of Dammer *et al* [5] on the same system, who report a transition at 18 at.% Ni. No significant structural changes were observed around this composition range and these would be expected if a traditional model of the MIT is applicable. However, the MIT lies within the two-phase region, so a percolation model is more appropriate. Percolation theory gives a MIT when the volume fraction of the conducting phase is about 16% [19]. Here, the conducting phase is amorphous NiSi. Taking the density of this material to be the same as that of the crystal (6700 kg m^{-3} [14]) and that of amorphous Si as 2300 kg m^{-3} we find that a volume fraction of 16% NiSi corresponds to $x = 0.16$. This is very close to the observed position of the MIT. The equality between x and the volume fraction is coincidental.

6. Conclusion

We have used optical spectroscopy to measure the extent of the band gap in a series of a-$Si_{1-x}Ni_x$ samples and found that around 13 at.% Ni was enough to induce a MIT. An EXAFS study undertaken on these samples shows an increase in the Si–Si bond length from 2.34 to 2.44 Å across this composition range ($0 \leqslant x \leqslant 0.50$). The same technique shows an invariant nickel environment in the same composition range. We interpret our structural results in terms of the appearance of a discrete a-Si:Ni phase rather than the interstitial occupancy or substitution of Si atoms by Ni in a TRN. Evidence is provided by a high Ni coordination, suggesting that Ni exists only in a close-packed alloy of Si–Ni, and a Si–Ni distance characteristic of this bond in c-NiSi. Further evidence is supplied by a complementary SAXS study which reveals the presence of two phases, probably a-Si and a-NiSi. Evidence for two phases in the a-$Si_{1-x}Ni_x$:H system has previously been reported [7, 9]. These results suggest that a percolation theory describing the connectivity of regions of a conducting a-Si:Ni alloy within an a-Si matrix is a more appropriate model of the MIT than the traditional Anderson model.

References

[1] Morigaki K 1980 *Phil. Mag.* **42** 979
[2] Mott N 1974 *Metal–Insulator Transitions* (London: Taylor and Francis)
[3] Regan M J, Rice M, Fernandez van Raap M B and Bienenstock A 1994 *Phys. Rev. Lett.* **73** 1118
[4] Colver M M 1977 *Solid State Commun.* **23** 333
[5] Dammer U, Adkins C J, Asal R and Davis E A 1993 *J. Non-Cryst. Solids* **166** 501
[6] Rogachev N A, Smid V, Mares J J and Kristofik J 1987 *J. Non-Cryst. Solids* **97/98** 955
[7] Edwards A M, Fairbanks M C, Newport R J, Gurman S J and Davis E A 1989 *J. Non-Cryst. Solids* **113** 41
[8] Asal R, Baker S H, Gurman S J, Bayliss S C and Davis E A 1992 *J. Phys.: Condens. Matter* **4** 7169
[9] Rigden J S and Newport R J 1999 *J. Mater. Res.* **14** 1272
[10] Gurman S J, Binsted N and Ross I 1984 *J. Phys. C: Solid State Phys.* **17** 143
[11] Joyner R W, Martin K J and Meehan P 1987 *J. Phys. C: Solid State Phys.* **20** 4005
[12] Guinier A and Fournet G 1955 *Small-Angle Scattering of X-Rays* (New York: Wiley)
[13] Wyckoff R W G 1971 *Crystal Structure* 2nd edn (New York: Interscience) p 1040
[14] Trotter J (ed) 1971 *Structure Reports for 1971 (Metals Inorganic Sections vol 15)* (Utrecht: Oosthoek, Scheltema and Holkema) p 107
[15] Bayliss S C and Gurman S J 1991 *J. Non-Cryst. Solids* **127** 174
[16] Cyrin S J 1968 *Molecular Vibrations and Mean Square Amplitudes* (Amsterdam: Elsevier)
[17] Kittel C 1971 *Introduction to Solid State Physics* 4th edn (London: Wiley) p 209
[18] Kittel C 1971 *Introduction to Solid State Physics* 4th edn (London: Wiley) p 219
[19] Zallen R 1983 *Physics of Amorphous Solids* (New York: Wiley)